

Supplementary Materials for
**Skeletal muscle NOX4 is required for adaptive responses that prevent
insulin resistance**

Chrysovalantou E. Xirouchaki, Yaoyao Jia, Meagan J. McGrath, Spencer Creatorex,
Melanie Tran, Troy L. Merry, Dawn Hong, Matthew J. Eramo, Sophie C. Broome,
Jonathan S. T. Woodhead, Randall F. D'souza, Jenny Gallagher, Ekaterina Salimova,
Cheng Huang, Ralf B. Schittenhelm, Junichi Sadoshima, Matthew J. Watt,
Christina A. Mitchell, Tony Tiganis*

*Corresponding author. Email: tony.tiganis@monash.edu

Published 15 December 2021, *Sci. Adv.* 7, eabl4988 (2021)
DOI: [10.1126/sciadv.abl4988](https://doi.org/10.1126/sciadv.abl4988)

This PDF file includes:

Figs. S1 to S14

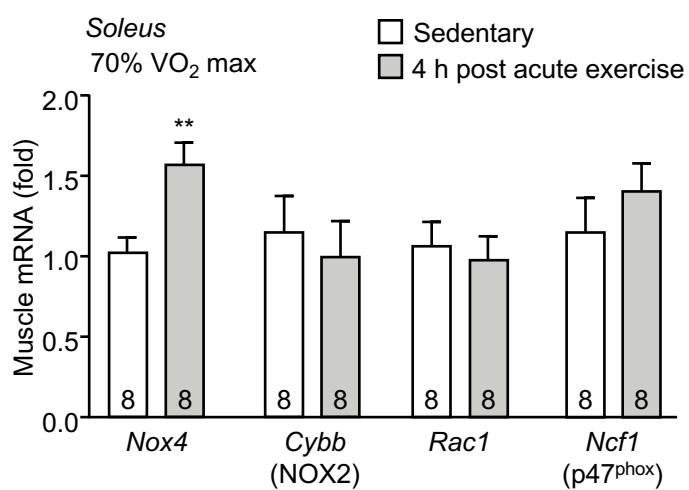
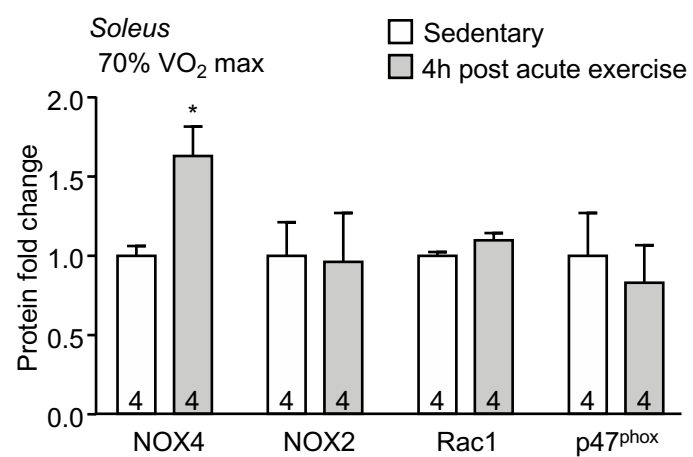
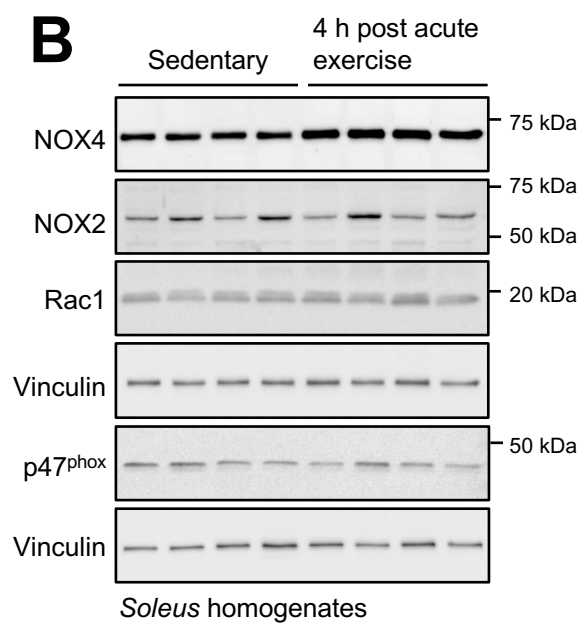
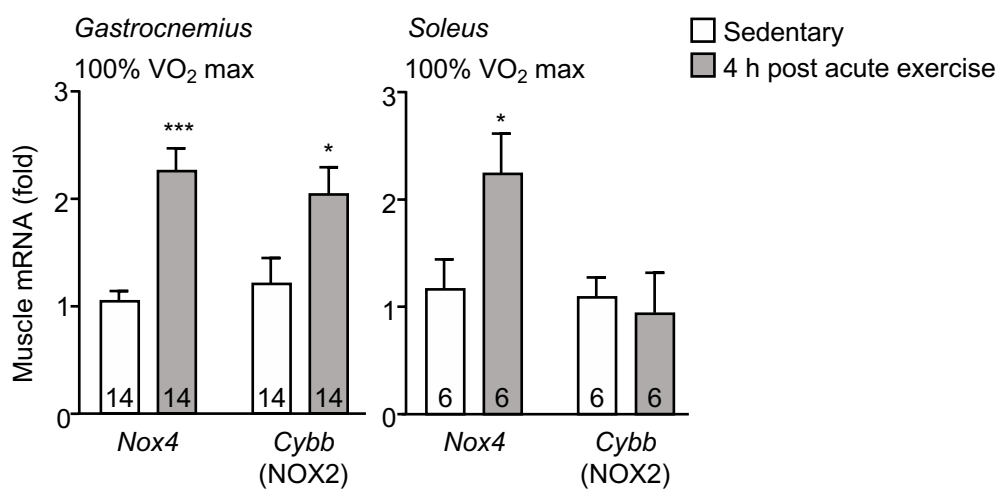
A**B****C**

Fig. S1. NOX4 is induced by exercise (Related to Fig. 1). 12-week-old C57BL/6 male mice were subjected to an acute bout of exercise on multi-lane treadmill for 50 min at moderate intensity (70% VO₂max). After 4 h tissues were collected from sedentary controls and exercised mice and *soleus* muscles processed for **a)** quantitative real time PCR (qPCR) and **b)** immunoblotting. 12-week-old C57BL/6 male mice were subjected to an acute bout of exercise on multi-lane treadmill for 50 min at high intensity (90-100% VO₂max). After 4 h, tissues were collected from sedentary controls and exercised mice and *gastrocnemius* and *soleus* muscles processed for **c)** qPCR. Representative and quantified results are shown (means ± SEM) for the indicated number of mice; significance determined using a Student's t-test.

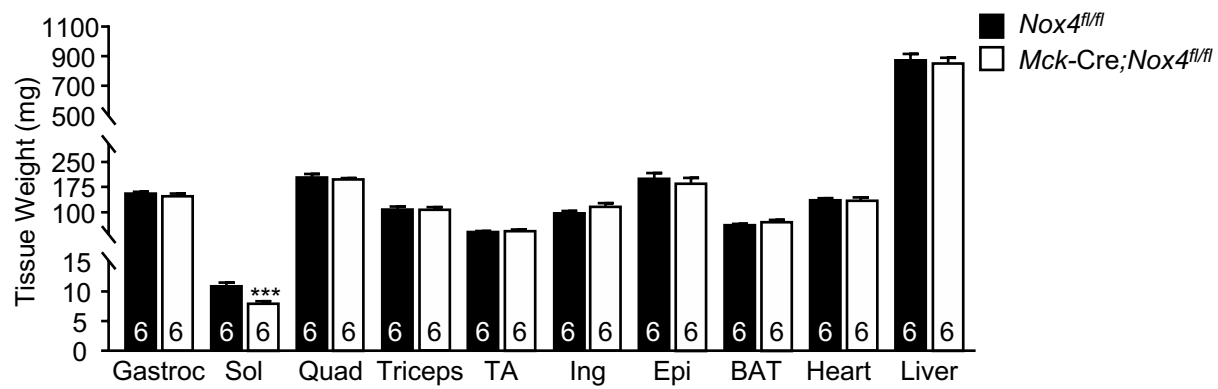
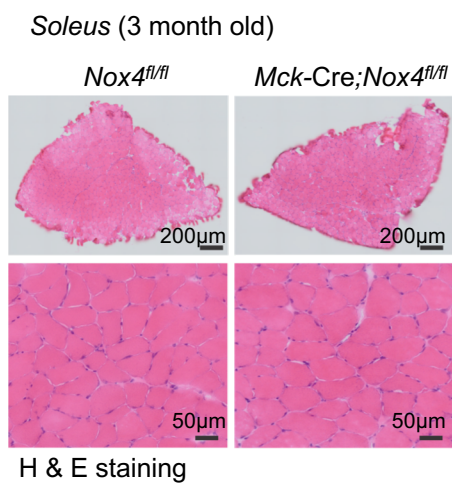
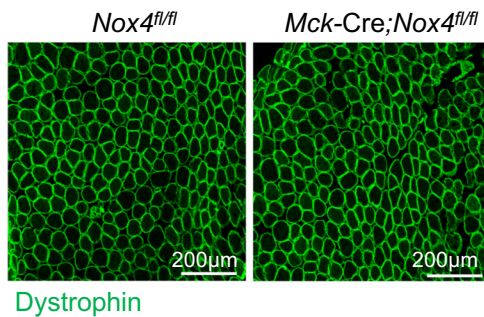
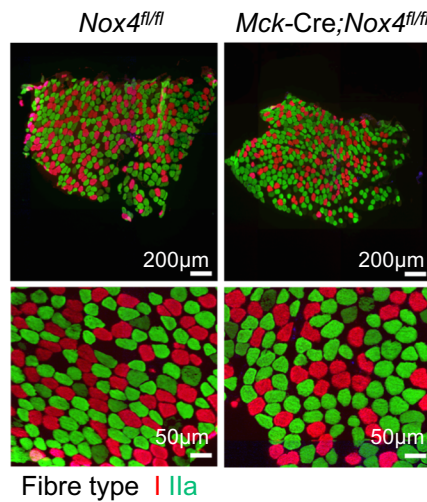
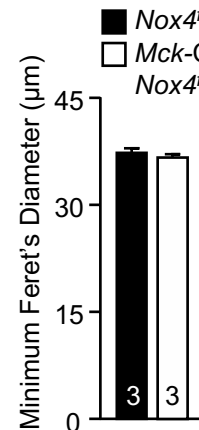
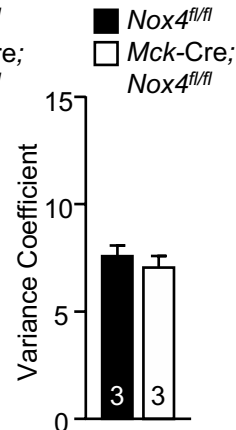
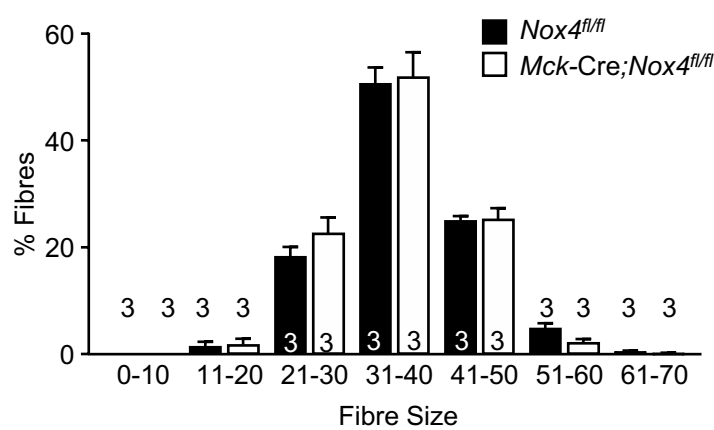
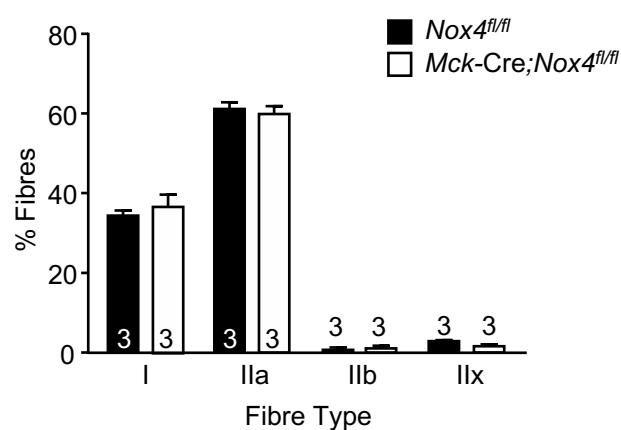
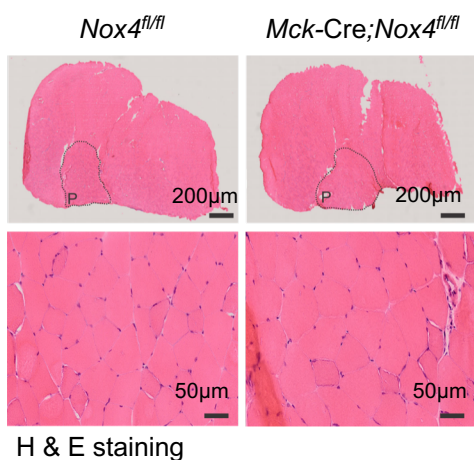
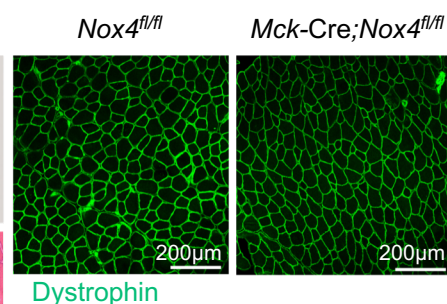
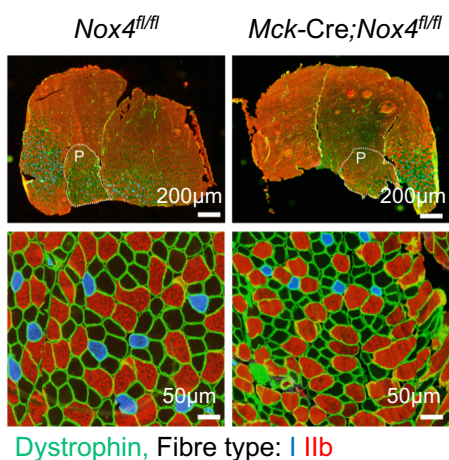
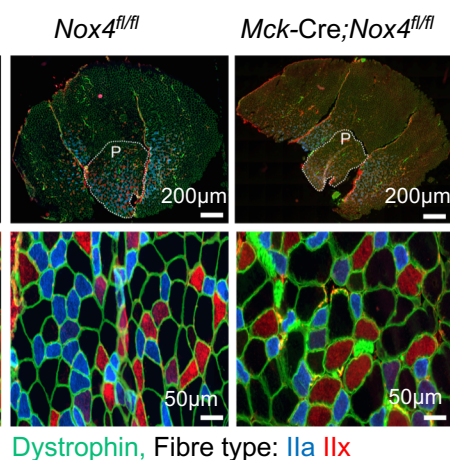
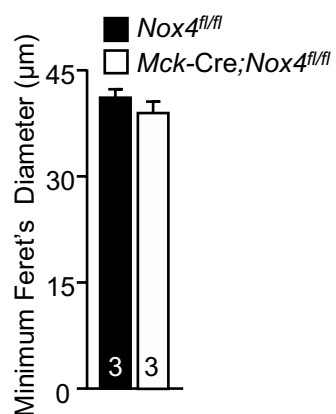
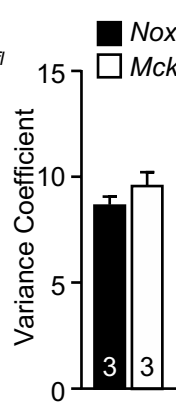
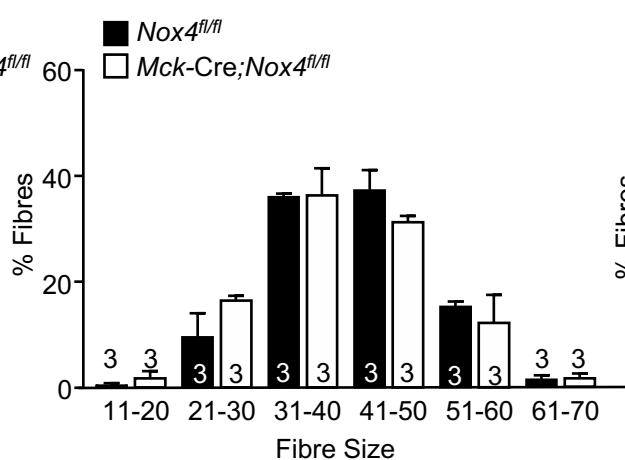
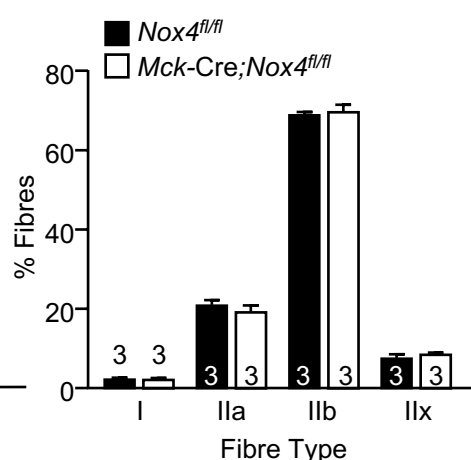
A**B****C****D****E****F****G****H****I***Gastrocnemius* (3 month old)**J****K****L****M****N****O****P**

Fig. S2. NOX4 deletion does not affect muscle development (Related to Fig. 1). a-q) 12-week-old *Nox4^{fl/fl}* and *Mck-Cre;Nox4^{fl/fl}* male mice were fed a standard chow diet. **a)** Tissues [including *gastrocnemius* (Gastroc), *soleus*, *quadriceps* (Quad), *triceps* and *tibialis anterior* (TA) skeletal muscles, epididymal (Epi) and inguinal (Ing) white adipose tissues, interscapular brown adipose tissue (BAT), heart and liver] were extracted and weighed. **b-p)** Transverse sections (10 nm) were prepared from frozen **b-h)** *soleus* and **i-p)** *gastrocnemius* muscles and stained with **b, i)** haematoxylin and eosin (H&E) or immunostained for **c, j)** dystrophin, or **d, k, l)** fibre types I, or IIa, IIb, IIx. For **k, l)** P represents the location of *plantaris* inside *gastrocnemius* muscle. **e, m)** The minimum Feret's diameter (closest distance between two parallel tangents of the muscle fibre perimeter), **f, n)** the variability coefficient (the standard deviation of the minimum Feret's diameter) and both **g, o)** fibre size and **h, p)** fibre types were determined. Representative and quantified results are shown (means \pm SEM) for the indicated number of mice.

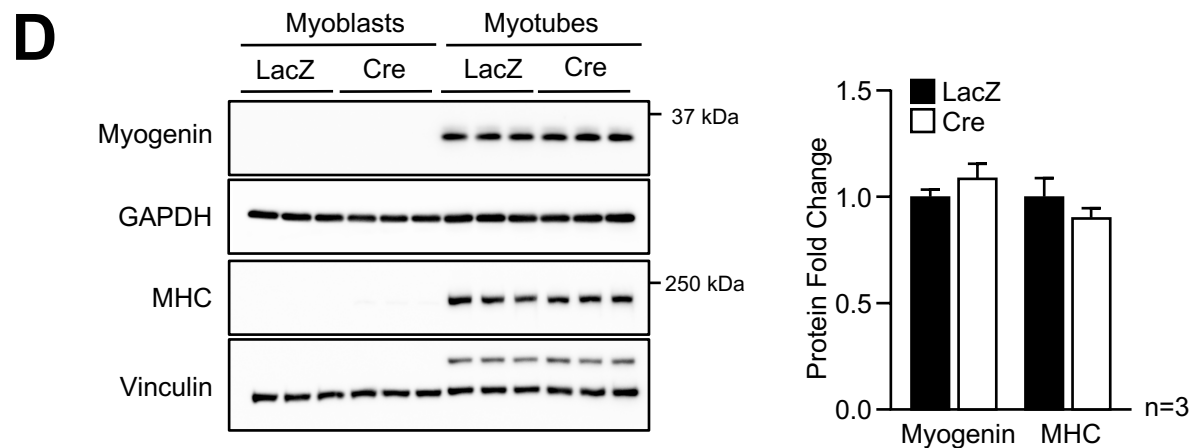
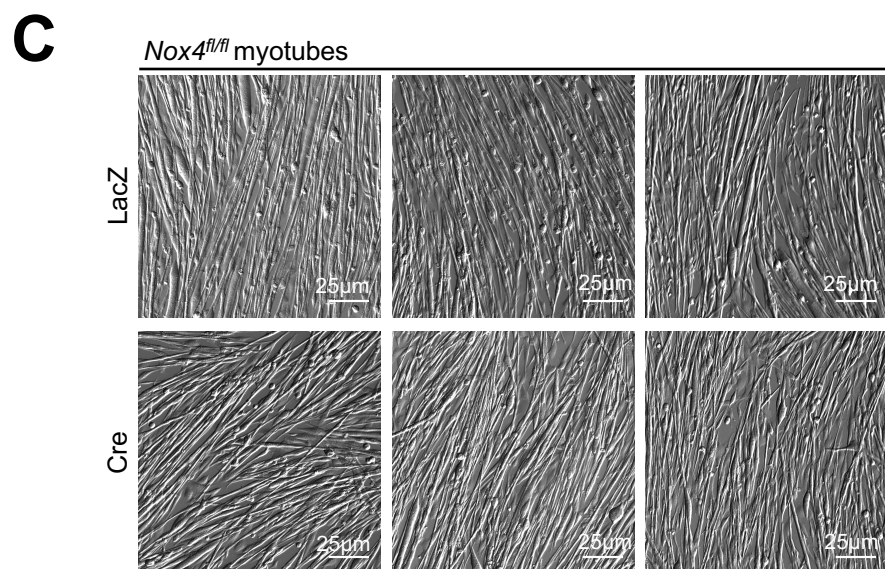
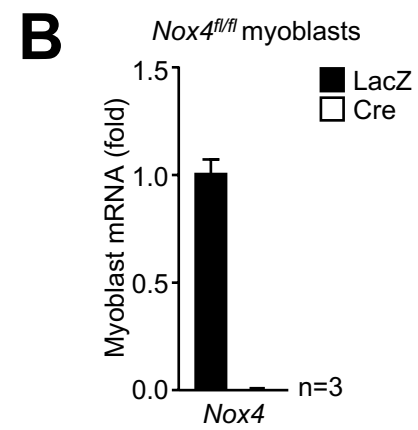
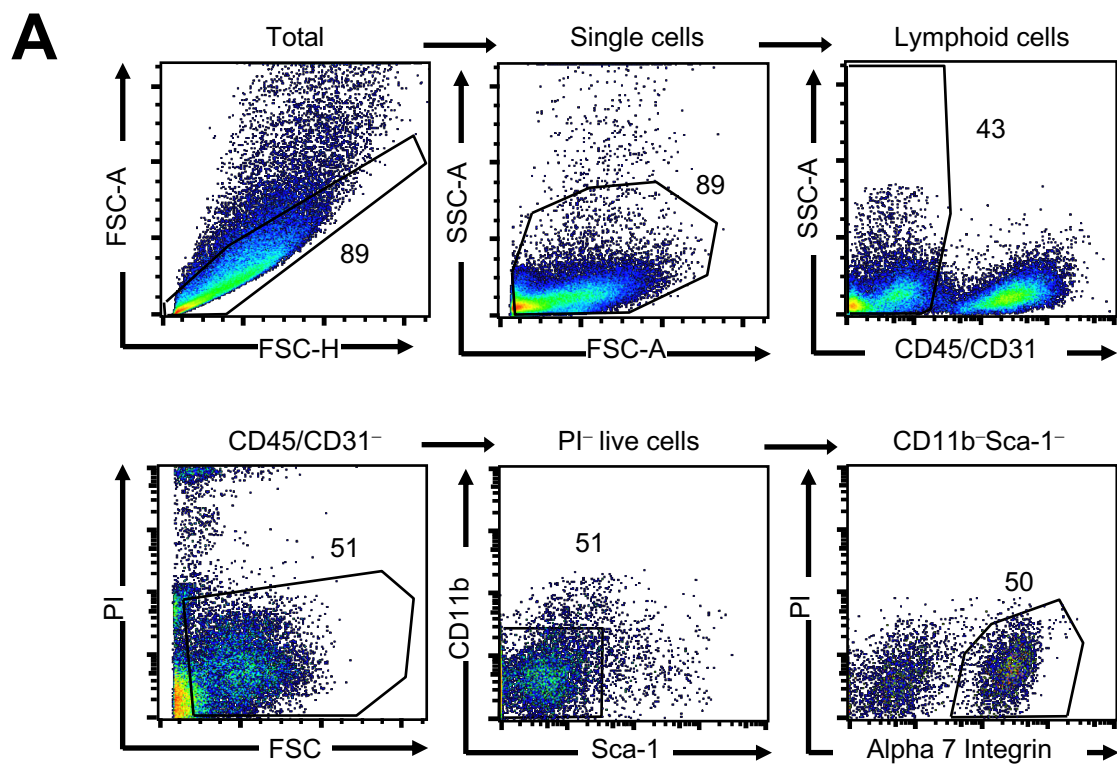


Fig. S3. Isolation and generation of NOX4-deficient muscle cells (Related to Fig. 2).

a) FACS gating strategy for *Nox4*^{fl/fl} myoblast isolation. Skeletal muscle was digested with collagenase D and dispase II and myoblasts stained with fluorophore-conjugated antibodies to CD45, CD31, CD11b, Sca1 and α 7-integrin. CD45⁻CD31⁻CD11b⁻Sca1⁻ α 7-integrin⁺ cells were purified by flow cytometry; dead cells were excluded with propidium iodide (PI). **b-g)** FACS-purified *Nox4*^{fl/fl} myoblasts were transduced with β -galactosidase (LacZ) control or Cre recombinase-expressing adenoviruses to delete *Nox4* and the resultant LacZ or Cre myoblasts used for further experiments. **b)** *Nox4* mRNA levels in myoblasts were assessed by qPCR. **c)** LacZ and Cre myoblasts were differentiated into myotubes. Myotube differentiation was assessed by brightfield microscopy; representative images are shown. **d)** Myotube differentiation was assessed by immunoblotting for myogenin and myosin heavy chain (MHC) proteins. In **d)** myotube micrographs derived from three independent adenoviral myoblast transductions are shown. In **(d)** individual lanes on immunoblots correspond to independent adenoviral transductions and cell isolations. Quantified results (means \pm SEM) are from the indicated number of independent adenoviral transductions and are representative of at least three independent experiments.

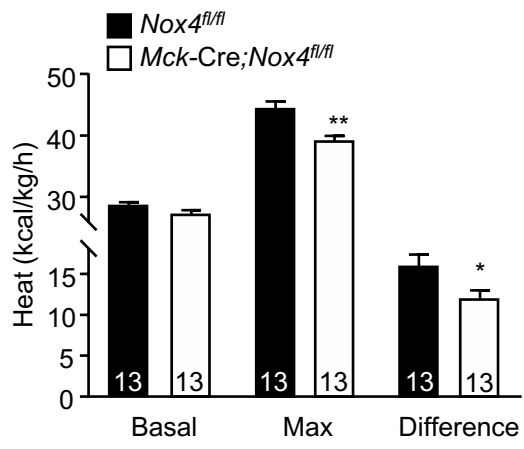
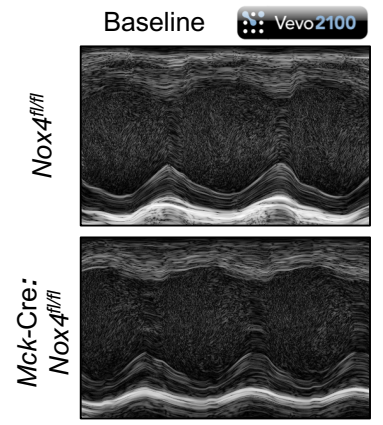
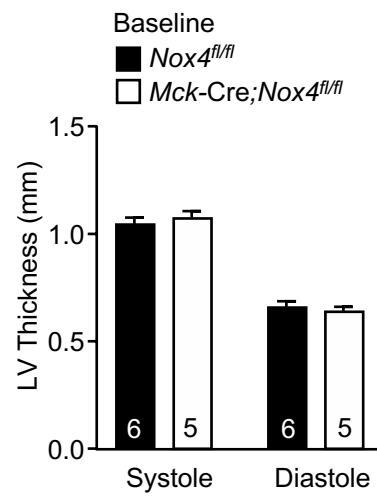
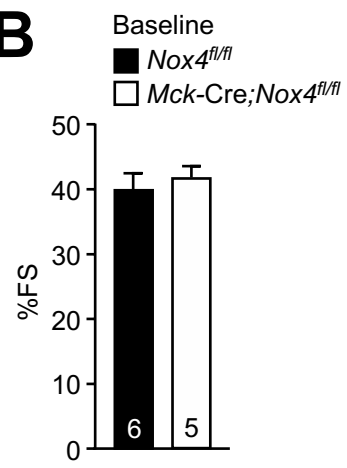
A**B**

Fig. S4. NOX4 deficiency in *Mck-Cre;Nox4^{fl/fl}* mice impairs exercise performance but not heart function (Related to Fig. 3). **a)** 12-week-old *Nox4^{fl/fl}* and *Mck-Cre;Nox4^{fl/fl}* male mice fed a chow-diet were subjected to an exercise-stress-test in an enclosed treadmill connected to a Comprehensive Lab Animal Monitoring System (CLAMS) for respiratory assessments and the determination of heat produced during exercise. **b)** 10-12-week-old *Nox4^{fl/fl}* and *Mck-Cre;Nox4^{fl/fl}* male mice fed a chow-diet were sedated and subjected to echocardiography. Fractional shortening (%FS) and left ventricle (LV) thickness assessed. Representative M-mode images were also acquired through a short-axis view at the papillary muscle level. Representative and quantified results are shown (means \pm SEM) for the indicated number of mice; significance in (a) determined using a two-way ANOVA.

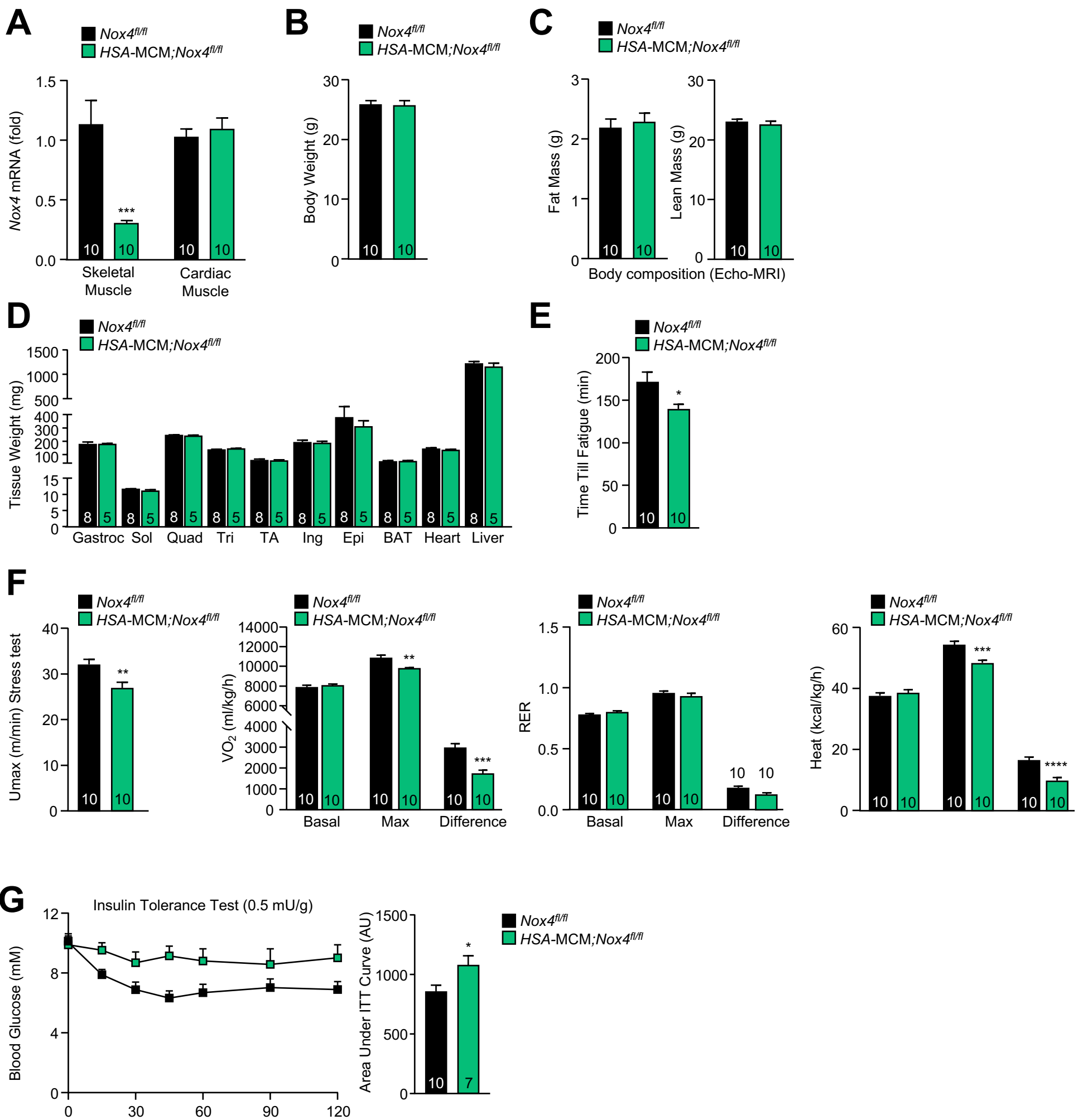


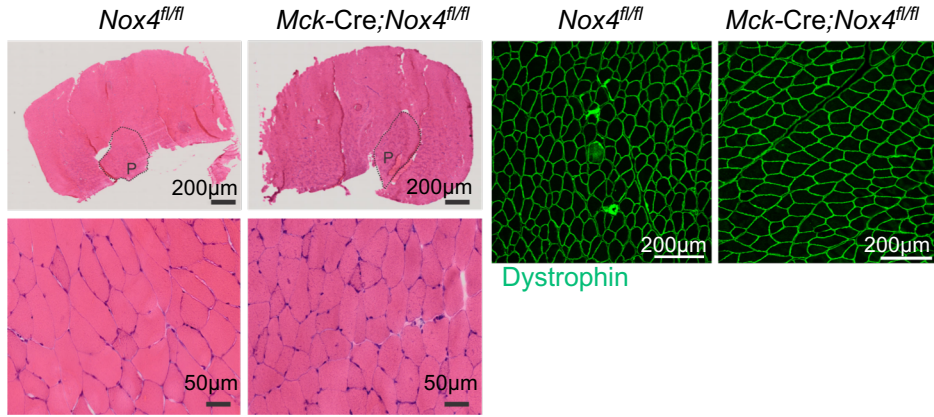
FIG S5

Fig. S5. NOX4 deletion in adult mice impairs exercise performance (Related to Fig. 3). a-g)

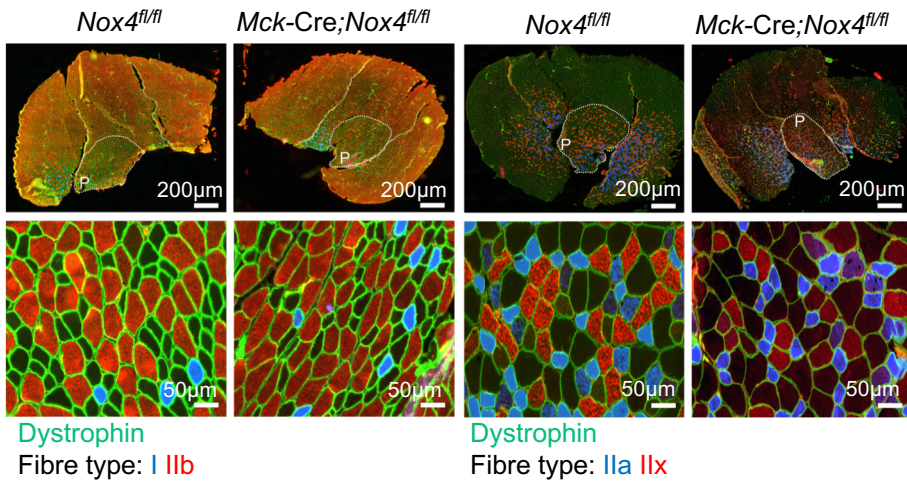
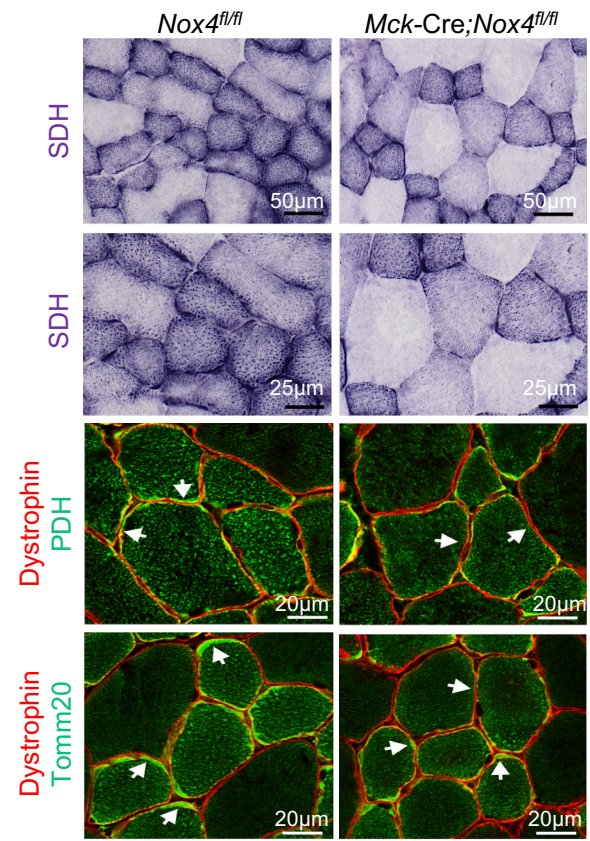
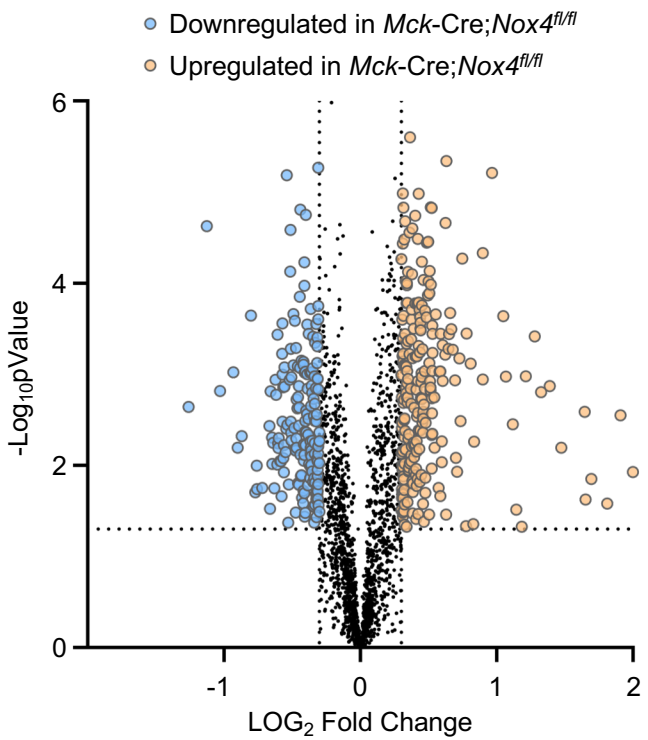
9-week-old *Nox4^{fl/fl}* and *HSA-MCM;Nox4^{fl/fl}* male mice fed a standard chow diet were treated with tamoxifen (80 mg/kg) for 5 consecutive days and analysed at 12 weeks. **a)** Cardiac muscle and *gastrocnemius* skeletal muscle were extracted for qPCR analysis to monitor *Nox4* mRNA levels. **b)** Body weight, **c)** body composition (Echo-MRI) and **d)** tissue weights [including *gastrocnemius* (Gastroc), *soleus*, *quadriceps* (Quad), *triceps* and *tibialis anterior* (TA) skeletal muscles, epididymal (Epi) and inguinal (Ing) white adipose tissues, interscapular brown adipose tissue (BAT), heart and liver] were determined. Mice were subjected to an **e)** endurance-test (time till fatigue assessed) and **f)** to an exercise-stress-test; U_{max} , VO_2 , RER and Heat were assessed. **g)** 9-week-old *Nox4^{fl/fl}* and *HSA-MCM;Nox4^{fl/fl}* male mice fed a standard chow diet were treated with tamoxifen (80 mg/kg) for 5 consecutive days and analysed at 24 weeks. Mice were subjected to insulin tolerance tests (ITTs; 0.5 mU insulin/g body weight); areas under ITT curves were determined and arbitrary units (AU) shown. Representative and quantified results are shown (means \pm SEM) for the indicated number of mice; significance determined using (a, e, f, g) a Student's t-test or (f) a two-way ANOVA.

A

Gastrocnemius (6 month old)



H & E staining

Dystrophin
Fibre type: I IIbDystrophin
Fibre type: IIa IIx**B****C****D**

Description	Dataset	NES	LOG qValue	qValue
PARKINSONS_DISEASE	KEGG	-2.615548	2.6928469	0.002028398
EUKARYOTIC_TRANSLATION_ELONGATION	REACTOME	-2.201789	2.6972294	0.002008032
ELECTRON_TRANSPORT_ATP_SYNTHESIS	REACTOME	-2.135653	2.6981005	0.002004008
OXIDATIVE_PHOSPHORYLATION	KEGG	-2.179283	2.6884198	0.00204918
CITRIC_ACID_CYCLE_TCA_CYCLE	REACTOME	-2.029972	2.705008	0.001972386
RESPIRATORY_ELECTRON_TRANSPORT	REACTOME	-1.914213	2.7118072	0.001941748
INTRINSIC_PATHWAY_FOR_APOPTOSIS	REACTOME	-2.012166	2.3988077	0.003992016
DETOXIFICATION_OF_REACTIVE_OXYGEN_SPECIES	REACTOME	-1.997586	1.3918169	0.004056795
METABOLISM_OF_XENOBIOTICS_BY_CYTOCHROME_P450	KEGG	-1.981983	2.3961994	0.004016064
ORGANELLE_BIOGENESIS_AND_MAINTENANCE	REACTOME	-1.968889	2.0977777	0.007984033
TP53_REGULATES_METABOLIC_GENES	REACTOME	-1.823334	2.1055101	0.007843139
PANCREATIC_CANCER	KEGG	-1.944564	2.0195317	0.009560229
STRIATED_MUSCLE_CONTRACTION	REACTOME	-1.841415	1.9111576	0.012269939
CARDIAC_MUSCLE_CONTRACTION	KEGG	-1.768391	1.7168377	0.019193859
GLUCONEOGENESIS	REACTOME	-1.771039	1.7151673	0.019267825
GLYOXYLATE_METABOLISM_AND_GLYCINE_DEGRADATION	REACTOME	-1.692105	1.6206565	0.023952095
MITOCHONDRIAL_FATTY_ACID_BETA_OXIDATION	REACTOME	-1.705057	1.5965971	0.025316455
GLUCOSE_METABOLISM	REACTOME	1.6644282	1.4259687	0.037500003
DNA_REPAIR	REACTOME	1.7058941	1.492185	0.03219697
NICOTINATE_AND_NICOTINAMIDE_METABOLISM	KEGG	1.6161077	1.5605897	0.027504915
ASSEMBLY_OF_COLLAGEN_FIBRILS	REACTOME	1.6711047	1.6038658	0.024896265
LAMININ_INTERACTIONS	REACTOME	1.9086984	1.8675517	0.01356589
EXTRACELLULAR_MATRIX_ORGANIZATION	REACTOME	1.8684741	1.8874298	0.012958962
MITOCHONDRIAL_TRANSLATION	REACTOME	1.775697	1.9921115	0.010183299
SIGNALING_BY_MET	REACTOME	2.0132172	2.2261701	0.005940594
ECM_RECEPTOR_INTERACTION	KEGG	2.0122113	2.4073909	0.003913894
MET_PROMOTES_CELL_MOTILITY	REACTOME	2.1562364	2.6981005	0.002004008

Fig. S6. Muscle development and proteomic analysis in 6 month-old *Mck-Cre;Nox4^{fl/fl}* mice (Related to Fig. 4). a-b) *Gastrocnemius* muscles from 6-month-old male *Nox4^{fl/fl}* and *Mck-Cre;Nox4^{fl/fl}* mice fed a chow diet (4.8% fat) were collected. **a)** Transverse sections (10 nm) were prepared from frozen *gastrocnemius* muscles and stained with haematoxylin and eosin (H&E) or co-immunostained for dystrophin, or fibre types (I, IIa, IIb, or IIx). **b)** Alternatively, transverse sections were processed for **f)** SDH staining and either PDH or Tomm20 immunostaining along with dystrophin immunostaining to define mitochondria within individual muscle fibres. **c-d)** *Gastrocnemius* muscle was homogenised and proteins digested with trypsin and analysed on a QExactive HF mass spectrometer. **c)** Volcano plot representation of differentially expressed muscle proteins between *Mck-Cre;Nox4^{fl/fl}* and *Nox4^{fl/fl}* mice considering a p-value and log2 fold-change cut-off of ≤ 0.05 and $> |0.3|$, respectively. Upregulated proteins in *Mck-Cre;Nox4^{fl/fl}* versus *Nox4^{fl/fl}* mice are shown in orange and downregulated proteins in blue. **d)** Differentially expressed proteins were subjected to a gene set enrichment analysis (GSEA). The table shows significantly regulated KEGG and Reactome pathways using a normalised enrichment score (NES) $>|1.5|$ and a qValue <0.05 .

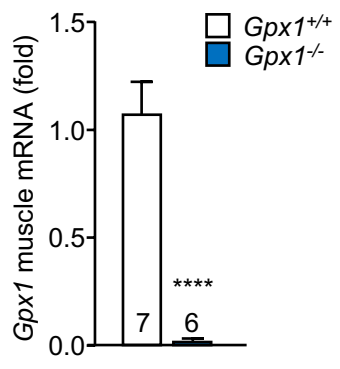
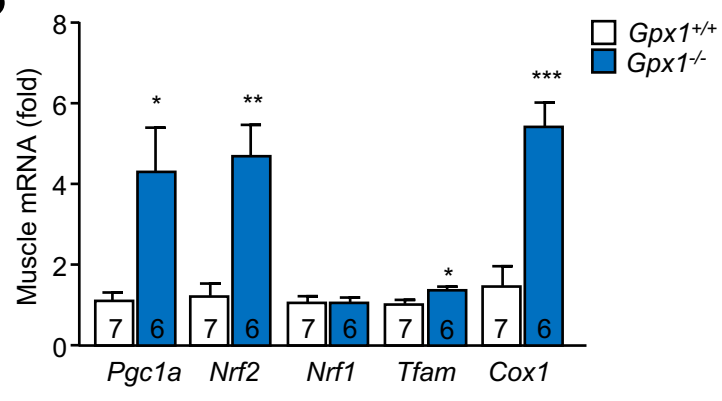
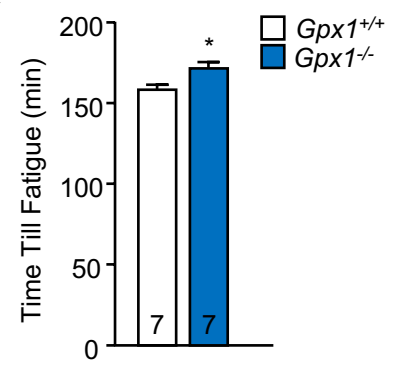
A**B****C**

Fig. S7. Improved mitochondrial biogenesis and endurance capacity in *Gpx1*^{-/-} mice
(Related to Fig. 4). **a-c)** 12-week-old *Gpx1*^{+/+} and *Gpx1*^{-/-} male mice were fed a chow diet (4.8% fat) and *gastrocnemius* muscle processed for qPCR to assess **a)** *Gpx1* and **b)** mitochondrial biogenesis gene expression. **c)** Mice were subjected to an endurance-test and the time until fatigue determined. Quantified results are shown (means ± SEM) for the indicated number of mice; significance determined using a Student's t-test.

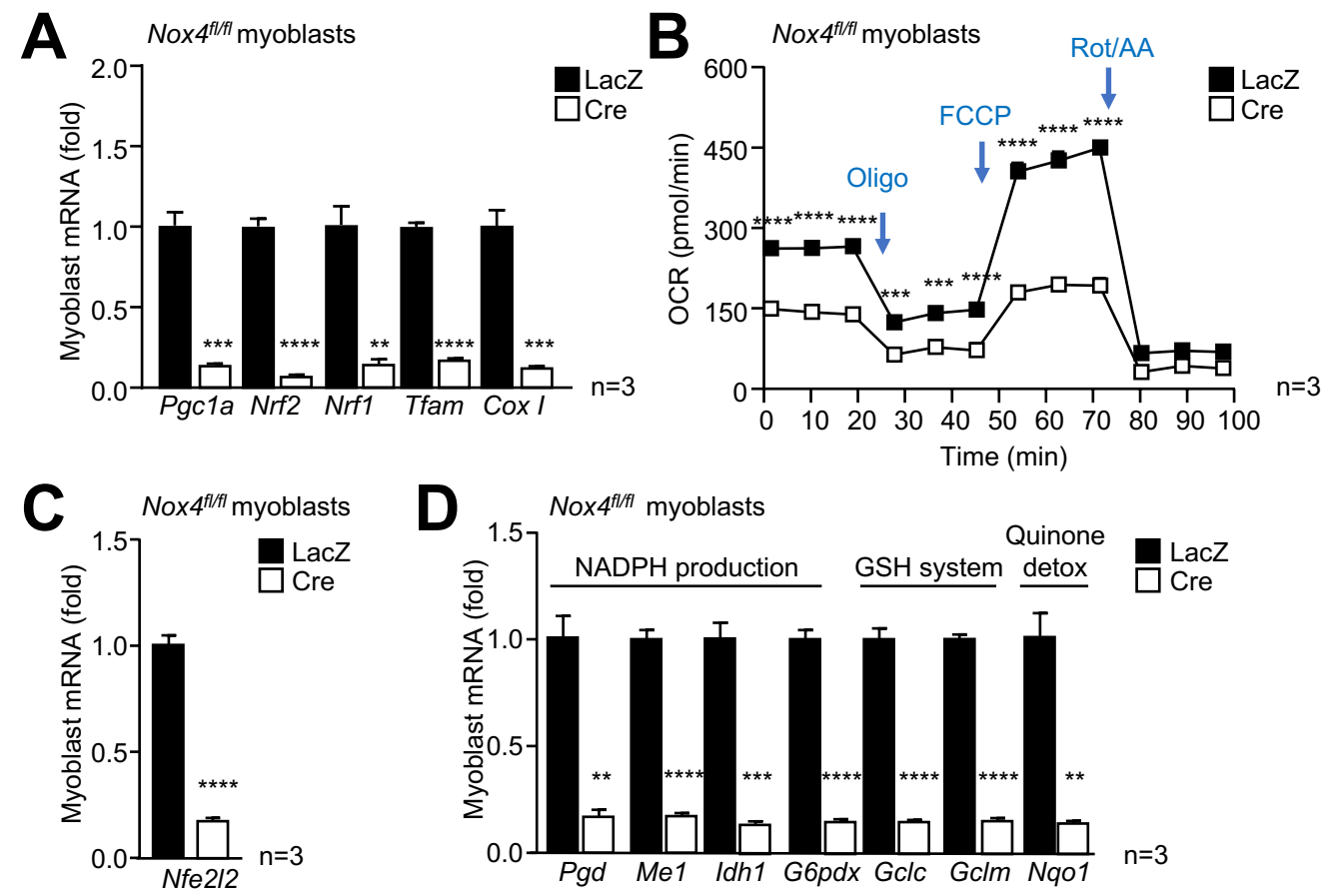


Fig. S8. Reduced mitochondrial biogenesis and antioxidant defence in NOX4-deficient myoblasts (Related to Fig. 5). **a-b)** FACS-purified *Nox4*^{fl/fl} myoblasts were transduced with β -galactosidase (LacZ) control or Cre recombinase-expressing adenoviruses to delete *Nox4*. **a)** The resultant LacZ or Cre myoblasts were processed for qPCR to assess the expression of mitochondrial biogenesis genes. **b)** Mitochondrial respiration was assessed in live myoblasts by performing a Seahorse XF Cell Mito Stress Test and measuring the oxygen consumption rate (OCR); basal and maximal respiration were assessed after inhibiting ATP synthase with oligomycin and uncoupling respiration with FCCP, **c-d)** LacZ or Cre myoblasts were processed for qPCR to assess the expression of antioxidant defence genes. Quantified results (means \pm SEM) are from the indicated number of independent adenoviral transductions and are representative of at least three independent experiments; significance was determined using a Student's t-test (a, c, d) or (b) a two-way ANOVA.

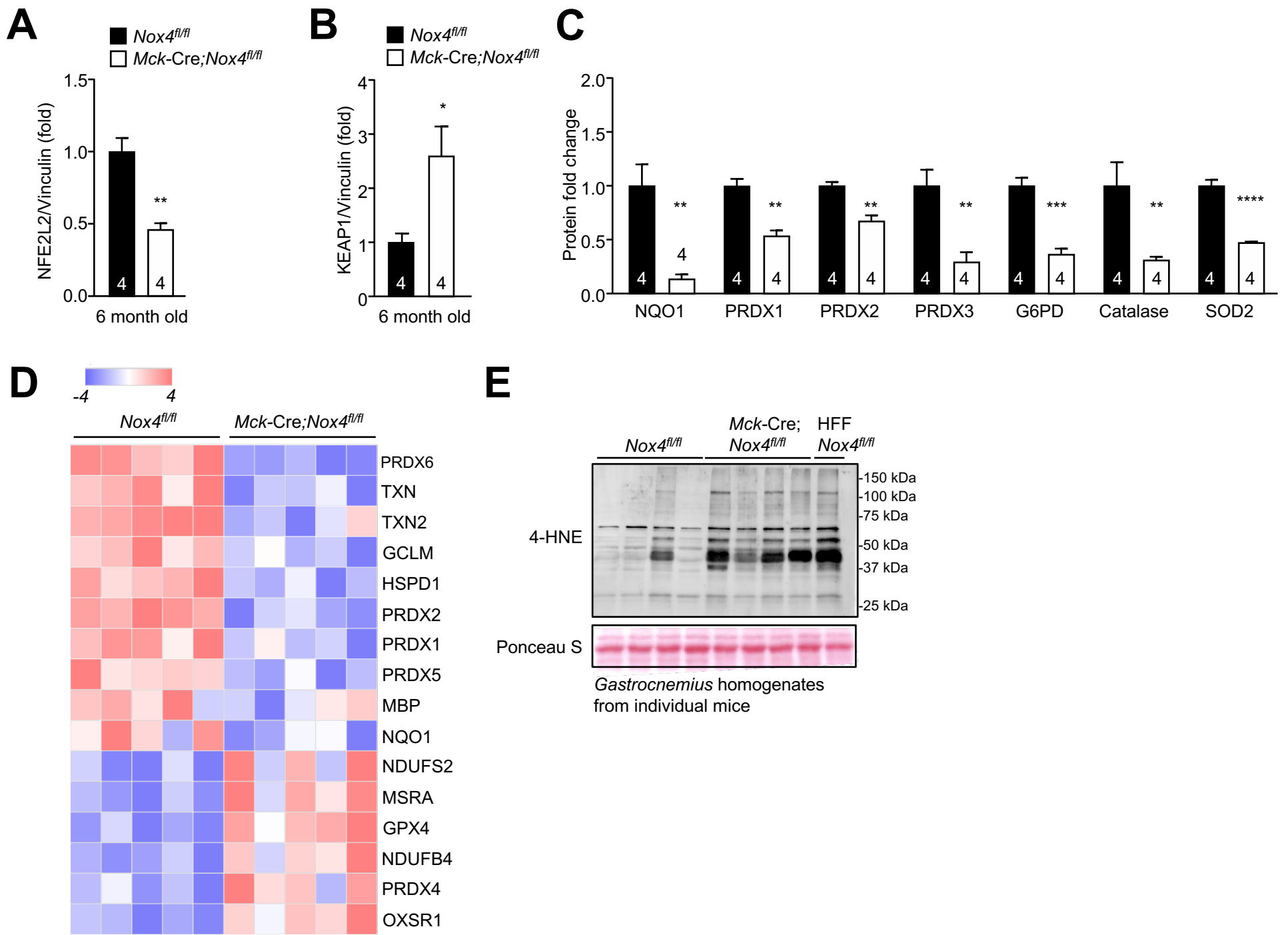


Fig. S9. Skeletal muscle NOX4 is essential for NFE2L2-mediated anti-oxidant defence (Related to Fig. 6). **a-c)** *Gastrocnemius* skeletal muscles from 6-month-old *Nox4^{fl/fl}* and *Mck-Cre;Nox4^{fl/fl}* male chow-fed were processed for immunoblotting. **a)** NFE2L2 and **b)** KEAP1 and antioxidant defence proteins were quantified by densitometry and normalised to vinculin (see **Fig. 6c**) or (see **Fig. 6e**). **d)** *Gastrocnemius* muscle from 6-month-old *Nox4^{fl/fl}* and *Mck-Cre;Nox4^{fl/fl}* male chow (4.8% fat)-fed mice was processed for proteomics analysis. A heatmap of significantly regulated proteins (\log_2 fold-change $> |1|$; p-value < 0.05 or FDR < 0.1) associated with the KEGG term “ROS Metabolism” is shown. **e)** *Gastrocnemius* skeletal muscle from 6-month-old *Nox4^{fl/fl}* and *Mck-Cre;Nox4^{fl/fl}* male chow-fed mice was processed for immunoblotting to assess 4-HNE levels and compared to that in 20-week high fat fed *Nox4^{fl/fl}* mice (last lane). Representative and quantified results are shown (means \pm SEM) for the indicated number of mice; significance was determined using Student’s t-test.

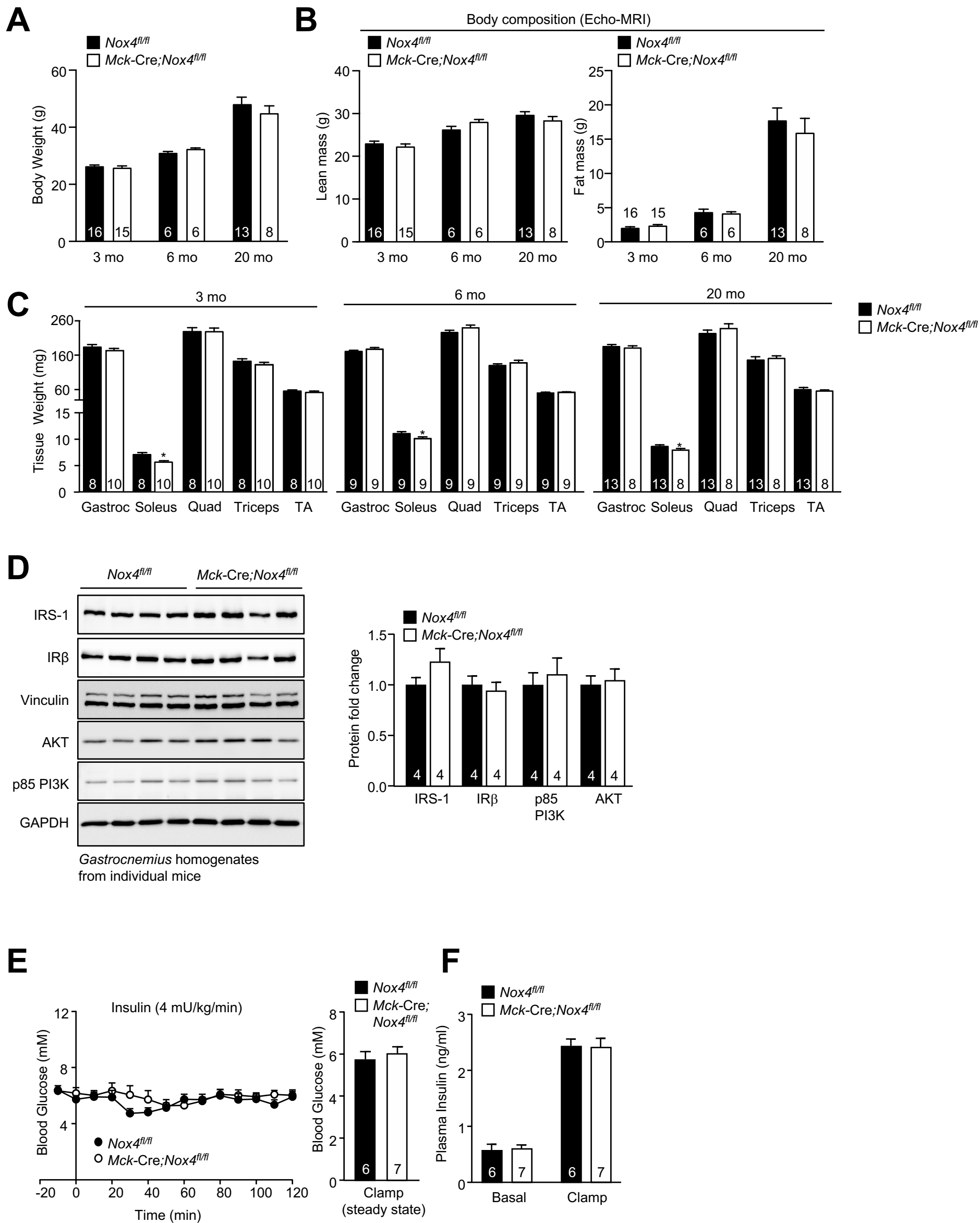


Fig. S10. Skeletal muscle NOX4-deficiency promotes insulin resistance in chow-fed mice without affecting body weight (Related to Fig. 7). **a)** Body weight, **b)** body composition (Echo-MRI) and **c)** skeletal muscle [*gastrocnemius* (Gastroc), *soleus*, *quadriceps* (Quad), *triceps* and *tibialis anterior* (TA)] tissue weights in 3-, 6- and 20-month-old *Nox4^{fl/fl}* and *Mck-Cre;Nox4^{fl/fl}* male chow-fed mice. **d)** *Gastrocnemius* skeletal muscle from 6-month-old *Nox4^{fl/fl}* and *Mck-Cre;Nox4^{fl/fl}* male chow-fed male mice was processed for immunoblotting; insulin receptor (IR) substrate-1 (IRS-1), IR β subunit (IR β), AKT and PI3K p85 subunit levels were quantified by densitometry and normalised to vinculin or GAPDH. **e-f)** 6-month-old male *Nox4^{fl/fl}* and *Mck-Cre;Nox4^{fl/fl}* male chow-fed mice were fasted for 6 h and conscious and unrestrained mice were subjected to hyperinsulinaemic-euglycaemic clamps. Blood glucose levels during the clamp as well as basal and clamped insulin levels were determined. Representative and quantified results are shown (means \pm SEM) for the indicated number of mice.

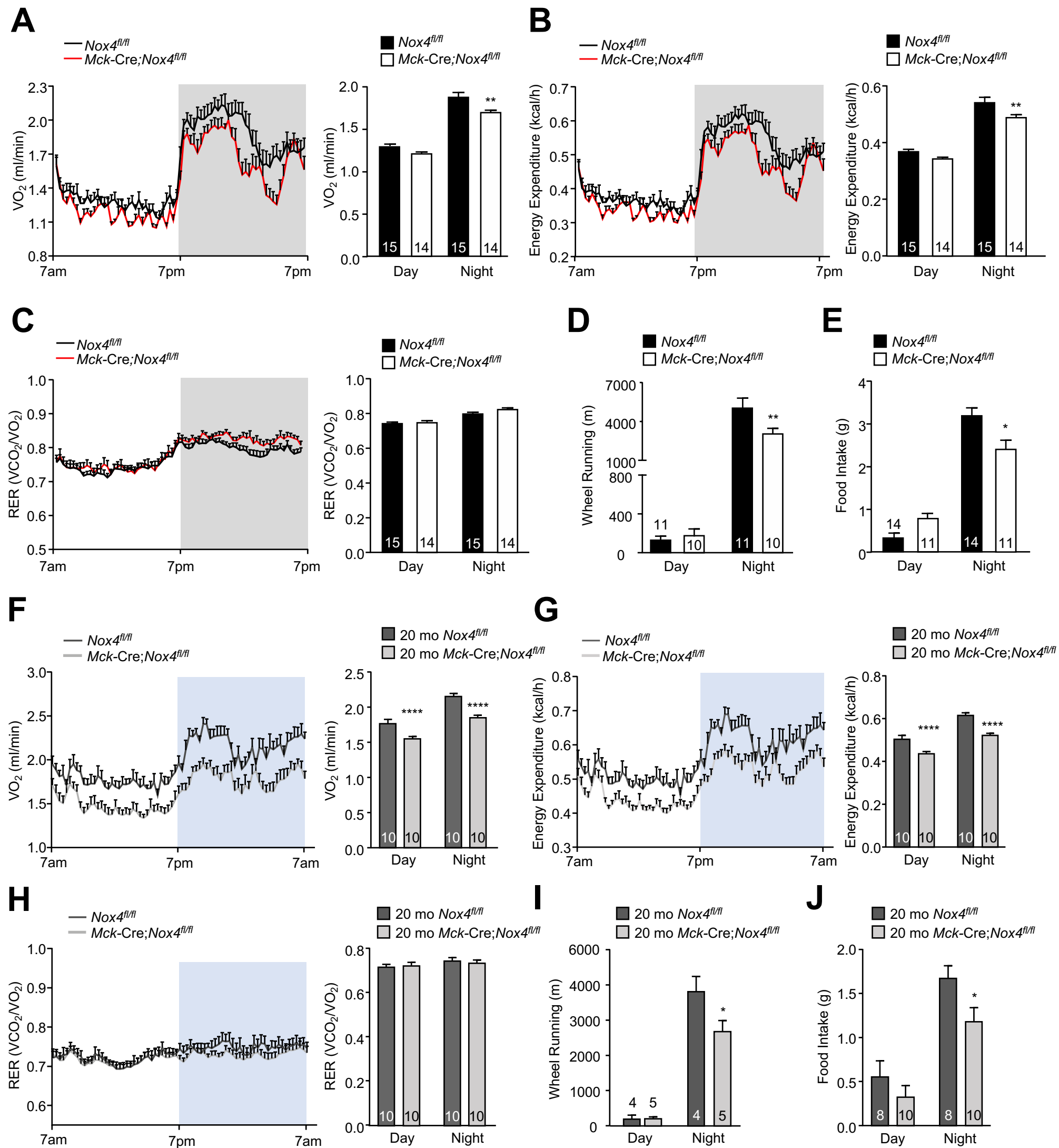


FIG S11

Fig. S11. NOX4 deletion in skeletal muscle reduces energy expenditure, wheel running and food intake (Related to Fig. 7). **a, f)** Oxygen consumption, **b, g)** energy expenditure, **c, h)** respiratory exchange ratio (RER), **d, i)** voluntary wheel running and **e, j)** diurnal food intake in **a-e)** 12-week-old and **f-j)** 20-month-old *Nox4^{fl/fl}* and *Mck-Cre;Nox4^{fl/fl}* chow-fed male mice. Quantified results are shown (means \pm SEM) for the indicated number of mice; significance determined using a-j) two-way ANOVA.

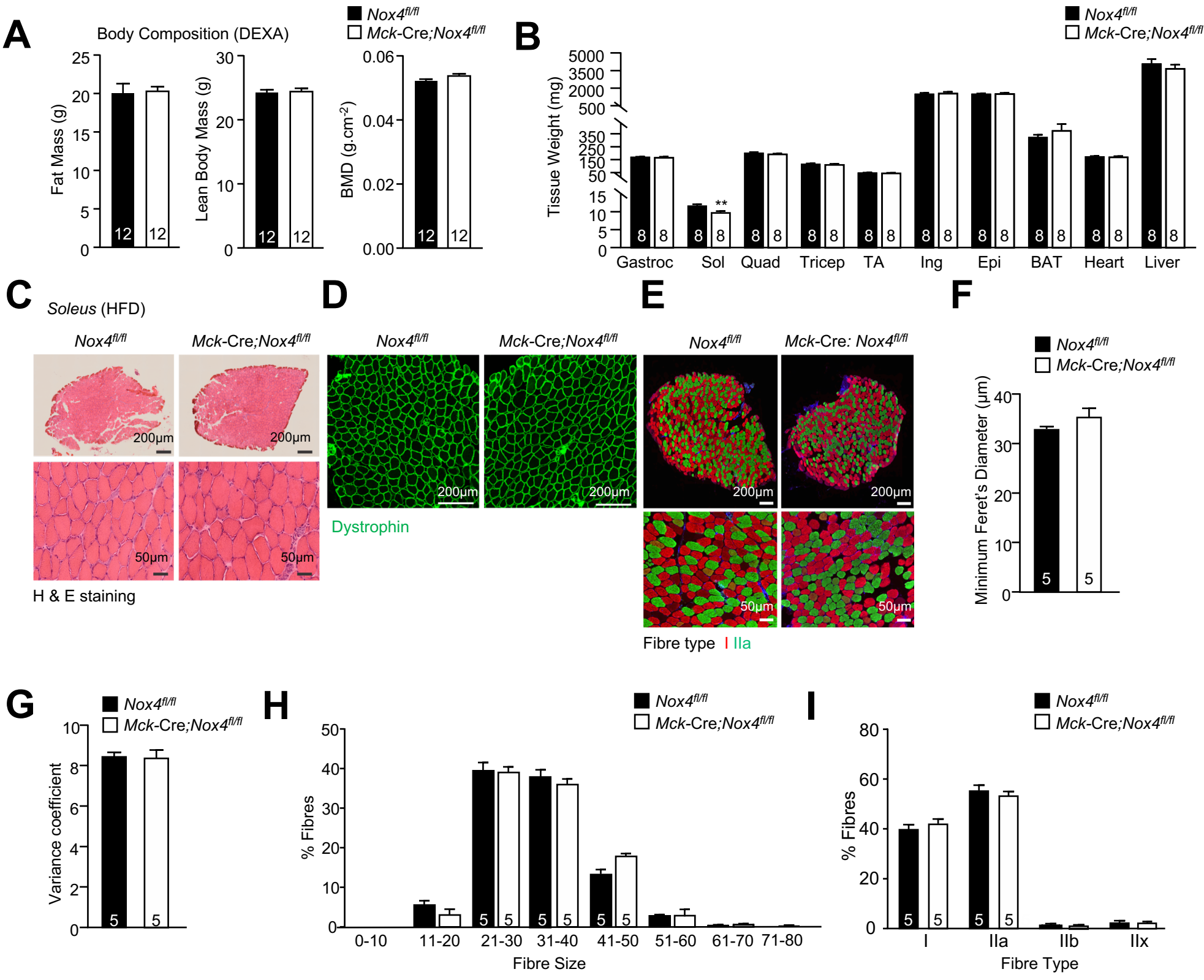


FIG S12

Fig. S12. *Nox4* deletion does not alter muscle development in obesity (Related to Fig. 8). **a-i)** 8-week-old *Nox4^{fl/fl}* and *Mck-Cre;Nox4^{fl/fl}* male mice were fed a high fat diet (HFD; 23% fat) for 20 weeks and **a)** body composition (DEXA) and **b)** tissue [including *gastrocnemius* (Gastroc), *soleus*, *quadriceps* (Quad), *triceps* and *tibialis anterior* (TA) skeletal muscles, epididymal (Epi) and inguinal (Ing) white adipose tissues, interscapular brown adipose tissue (BAT), heart and liver] weights were determined. **c-i)** Transverse sections (10 nm) were prepared from frozen soleus muscle and stained with **c)** haematoxylin and eosin (H&E) or immunostained for **d)** dystrophin, or **e)** co-immunostained for dystrophin and fibre type (I and IIa) and **f)** the minimum Feret's diameter, **g)** the variability coefficient and both **h)** fibre size and **i)** fibre types were determined. Representative and quantified results are shown (means \pm SEM) for the indicated number of mice.

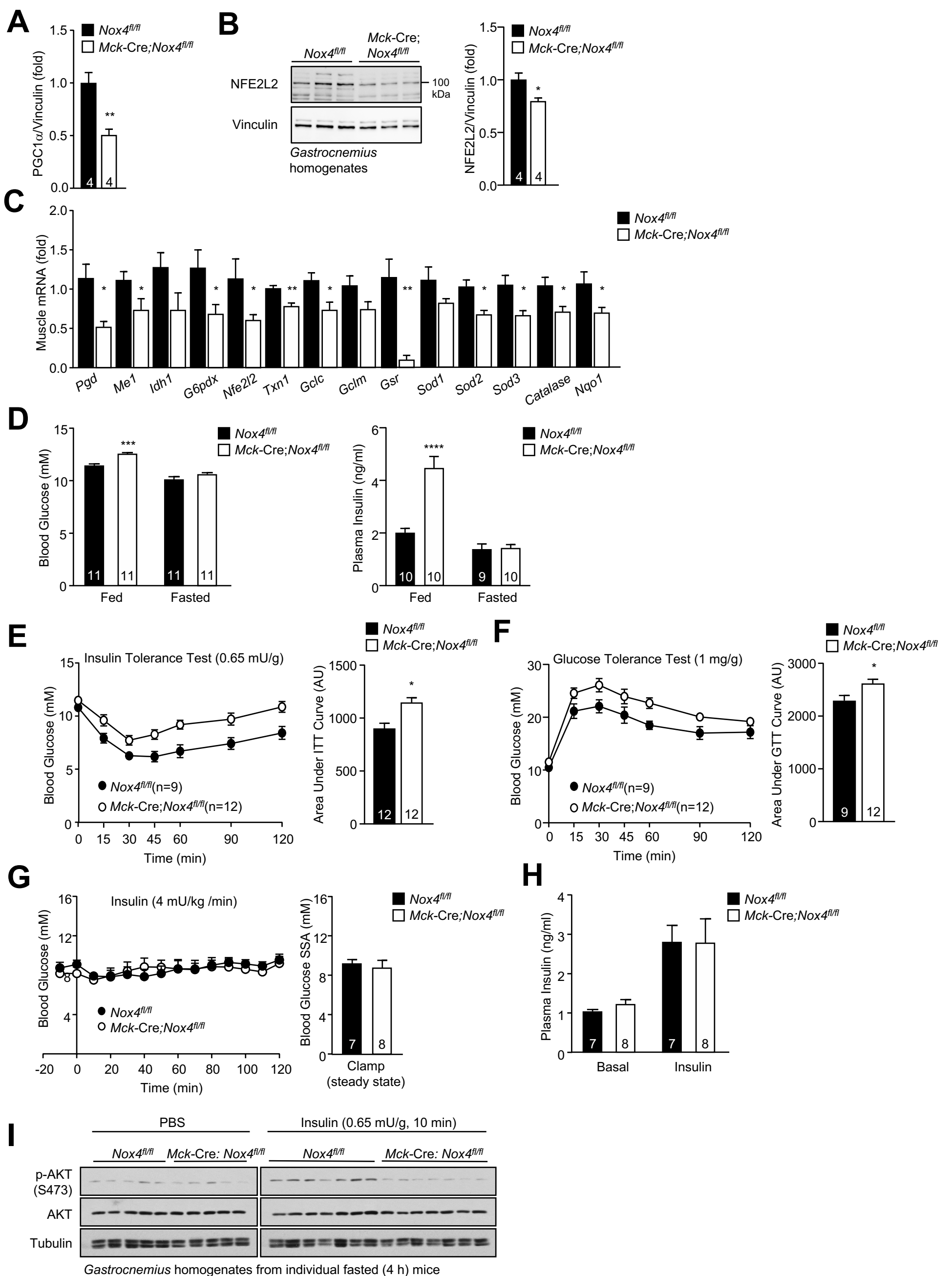


FIG S13

Fig. S13. *Nox4* deletion in muscle exacerbates obesity-associated insulin resistance (Related to Fig. 8). **a-c)** 8-week-old *Nox4^{fl/fl}* and *Mck-Cre;Nox4^{fl/fl}* male mice were fed a high fat diet (23% fat) for 20 weeks. *Gastrocnemius* muscle was processed for **a-b)** immunoblotting. **a)** PGC1 α protein levels quantified via densitometry (See **Fig. 8h**). **b)** NFE2L2 protein levels were assessed and quantified via densitometry. **c)** *Gastrocnemius* muscle was processed for qPCR to assess antioxidant defence gene expression. **d-h)** 8-week-old *Nox4^{fl/fl}* and *Mck-Cre;Nox4^{fl/fl}* male mice were fed a high fat diet (23% fat) for 20 weeks and **d)** fed (satiated; 11 pm) and fasted (6 h) blood glucose levels and insulin levels were assessed. Mice were subjected to **e)** insulin tolerance tests (ITTs; 0.65 mU insulin/g body weight) and **f)** glucose tolerance tests (GTTs; 1 mg glucose/g body weight); areas under ITT and GTT curves were determined and arbitrary units (AU) shown. **g-h)** After a 6 h fast, conscious and unrestrained mice were subjected to hyperinsulinaemic-euglycaemic clamps. **g)** Blood glucose levels during the clamp and **h)** basal and clamped insulin levels were determined. **i)** 8-week-old *Nox4^{fl/fl}* and *Mck-Cre;Nox4^{fl/fl}* male mice were fed a high fat diet (23% fat) for 12 weeks, fasted for 6 h and administered insulin (0.65 mU/g insulin intraperitoneal). *Gastrocnemius* muscle was extracted after 10 min and processed for immunoblotting. Representative and quantified results are shown (means \pm SEM) for the indicated number of mice; significance determined using (a-f) a Student's t-test.

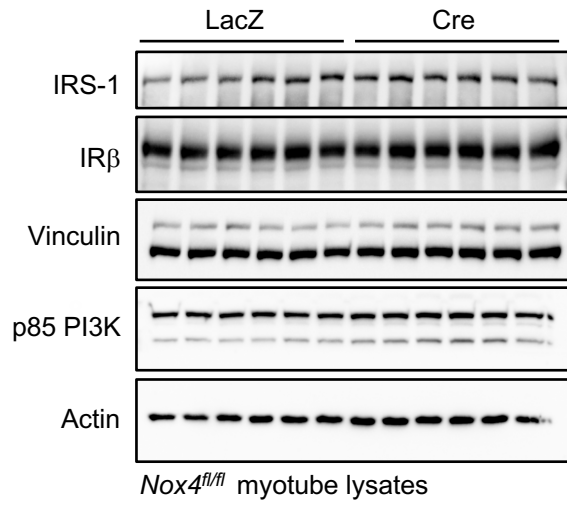
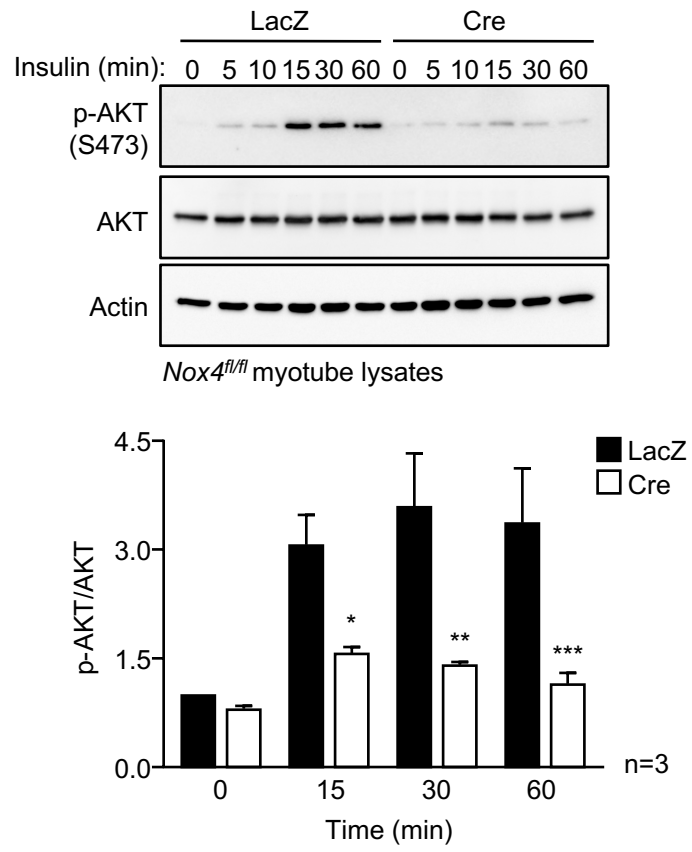
A**B**

Fig. S14. Diminished insulin signalling in NOX4-deficient myotubes (Related to Fig. 9).

FACS-purified *Nox4^{fl/fl}* myoblasts were transduced with β -galactosidase (LacZ) or Cre-expressing (Cre) adenoviruses and differentiated into myotubes. **a)** LacZ or Cre myotubes were processed for immunoblotting. **b)** LacZ or Cre myotubes were serum-starved (6 h) and either left unstimulated or stimulated with 1 nM insulin for the indicated time points and processed for immunoblotting. Representative and quantified results are shown (means \pm SEM) for the indicated number of experiments; significance determined using (b) a two-way ANOVA.